



HAL
open science

Akhmediev Breather dynamics and the nonlinear modulation instability spectrum

G. Genty, F. Dias, B. Kibler, N. Akhmediev, J.M. Dudley

► **To cite this version:**

G. Genty, F. Dias, B. Kibler, N. Akhmediev, J.M. Dudley. Akhmediev Breather dynamics and the nonlinear modulation instability spectrum. SPIE Photonics Europe : Conference on Nonlinear Optics and Applications, Apr 2010, Bruxelles, Belgium. 10.1117/12.854045 . hal-00606973

HAL Id: hal-00606973

<https://hal.science/hal-00606973v1>

Submitted on 17 Apr 2021

HAL is a multi-disciplinary open access archive for the deposit and dissemination of scientific research documents, whether they are published or not. The documents may come from teaching and research institutions in France or abroad, or from public or private research centers.

L'archive ouverte pluridisciplinaire **HAL**, est destinée au dépôt et à la diffusion de documents scientifiques de niveau recherche, publiés ou non, émanant des établissements d'enseignement et de recherche français ou étrangers, des laboratoires publics ou privés.



Distributed under a Creative Commons Attribution 4.0 International License

Akhmediev Breather dynamics and the nonlinear modulation instability spectrum

Goëry Genty^a, Frederic Dias^b, Bertrand Kibler^c, Nail Akhmediev^d, John M. Dudley^e

^aTampere University of Technology, Optics Laboratory, FI-33101 Tampere, Finland

^bCentre de Mathématique et de Leurs Applications (CMLA), ENS Cachan, France

^cCNRS/Université de Bourgogne, Institut Carnot de Bourgogne, 21078 Dijon, France

^dAustralian National University, Institute of Advanced Studies, Canberra ACT 0200, Australia

^eUniversité de Franche-Comté, Institut FEMTO-ST, 25030 Besançon, France

ABSTRACT

We consider various aspects of supercontinuum generation in the quasi-CW regime through analysis, numerical simulations and experiments. A new interpretation of certain features of the developing spectrum in terms of localized periodic structures known as “Akhmediev Breathers” is proposed. We also briefly consider the role of breather collisions and turbulence in the presence of higher order dispersion and show that they lead to the formation of very large amplitude localized structures that may be analogous to the infamous oceanic rogue waves.

Keywords: Solitons, nonlinear optics, supercontinuum generation, photonic crystal fiber, rogue waves.

1. INTRODUCTION

There has recently been much interest in the study of “rogue” events in nonlinear fiber optics [1-3]. Interest in this area began in 2007 with reports of extreme value soliton statistics during supercontinuum generation [1]. Although many aspects of fibre SC generation are now well-understood [4,5] these recent results have shown how noise-induced fluctuations in the long pulse quasi-CW regime can modify the dynamics so as to lead to very rare cases where high amplitude “optical rogue waves” are generated. These experiments attracted attention because they were carried out in a regime where spectral broadening was seeded by modulation instability (MI), allowing important links to be made with proposed formation mechanisms of oceanic rogue waves. The degree to which MI seeds either high power optical solitons or oceanic rogue waves is a subject of ongoing research, but insights into both optical and oceanic nonlinear propagation have already been obtained. In this regard, although the initial description of optical rogue waves was applied to rare high amplitude soliton pulses generated on the long-wavelength edge of a broadband fibre SC spectrum, there has recently been an improved understanding that a more likely analogy with the oceanic case is to be found in the onset phase of supercontinuum generation when coherent breather structures begin to emerge [6, 7].

This realization has led to the “rediscovery” by the optics community of powerful *analytic* solutions that rigorously describe induced MI and ultrashort pulse train formation from an initial beat signal. Although previous studies of this process have used numerical simulations or truncated sideband models, we show that the rediscovered 1985 “Akhmediev Breather” (AB) model provides an exact formalism with which to interpret this evolution [8]. In fact, despite intensive research over three decades, there are surprisingly-few analytic solutions describing nonlinear pulse evolution in optical fibers. Certainly there are exceptions such as the well-known soliton and self-similar solutions [9], but complex processes such as supercontinuum generation have generally been considered to require numerical approaches. In this paper, however, we summarize recent results that have shown that an analytic theory of “Akhmediev Breather” (AB) propagation can be successfully applied to quantitatively explain the form of the developing SC spectrum under long-pulse excitation conditions [10, 11]. Note that this present paper both summarizes the results in these previous works but also provides some additional unified and updated discussion in terms of other recent work we have carried out linking these ideas to the notion of soliton turbulence [12]. We show that the AB theory provides new insight into the properties of the initial broadening and nonlinear spectral transformation of CW supercontinuum generation seeded by noise. We discuss how the temporal structure that develops from spontaneous modulation instability (MI) can be naturally interpreted in terms of the characteristics of AB evolution, and we show how the frequency-domain properties of the

maximally-compressed AB solution reproduce the characteristic triangular shape of the MI spectrum when plotted on a semi-logarithmic scale. Numerical and analytic results are confirmed by experimental studies of quasi-CW spectral broadening induced by nanosecond pulse pumping in the anomalous dispersion regime of a photonic crystal fiber (PCF). Finally, we present simulations that go beyond the initial phase of AB evolution in the presence of symmetry-breaking third-order dispersion. We show that this leads to collisions and interactions between the emergent localized AB structures that may provide a natural link to the instabilities that occur in an oceanographic context.

2. THEORY

The AB theory we present here was developed in mid-1980s by Akhmediev and co-workers who used an insightful analytical approach to construct novel solutions to the nonlinear Schrodinger equation describing fiber propagation. This work has already been summarized by us in [10] but we re-present it here again for completeness. We first write the NLSE in dimensional form [4]:

$$i \frac{\partial A}{\partial z} + \frac{\beta_2}{2} \frac{\partial^2 A}{\partial T^2} + \gamma |A|^2 A = 0, \quad (1)$$

where $|A|^2$ has dimensions of instantaneous power in W and the dispersion and nonlinearity coefficients β_2 (< 0) and γ have dimensions of $\text{ps}^2 \text{ km}^{-1}$ and $\text{W}^{-1} \text{ km}^{-1}$ respectively. The AB solution describes the evolution along the propagation direction z of a wave with initial constant amplitude on which is superimposed a T -dependent low amplitude modulation. The solution then consists of an evolving train of pulses that is periodic in T and that exhibits periodic recurrence in z .

In contrast to soliton solutions which are localized in T , the ideal breather solution is localised in the z direction. In fact, certain initial conditions can also yield periodic evolution along the z -direction, but even in this case, the pulse train characteristics nonetheless remain well-described by the analytic AB solution. The AB solution to Eq. (1) is:

$$A(z, T) = \sqrt{P_0} \frac{(1-4a) \cosh(bz) + ib \sinh(bz) + \sqrt{2a} \cos(\omega_{\text{mod}} T)}{\sqrt{2a} \cos(\omega_{\text{mod}} T) - \cosh(bz)}, \quad (2)$$

which shows growth-return evolution over $-\infty < z < \infty$. The variable independent parameter ω_{mod} is the (perturbation) frequency of the initial temporal modulation. Coefficients a and b depend on ω_{mod} , defined by: $2a = [1 - (\omega_{\text{mod}}/\omega_c)^2]$ and $b = [8a(1-2a)]^{1/2}$ with $\omega_c^2 = 4\gamma P_0/|\beta_2|$ and P_0 the CW power at large $|z|$. The solution is valid over modulation frequencies that experience MI gain: $\omega_c > \omega_{\text{mod}} > 0$ such that a varies in the interval $0 < a < 1/2$ while the parameter $b > 0$ governs the MI growth. Maximum gain $b = 1$ occurs for $a = 1/4$, i.e. $\omega_{\text{mod}} = \omega_c/\sqrt{2}$. The solution in Eq. (2) describes an evolving periodic train of ultrashort pulses with temporal period $T_{\text{mod}} = 2\pi/\omega_{\text{mod}}$. The individual temporal sub-pulses have maximum amplitude and minimum temporal width at $z = 0$. The solution here describes the ‘‘maximally-compressed’’ AB:

$$A(z=0, T) = \sqrt{P_0} \frac{(1-4a) + \sqrt{2a} \cos(\omega_{\text{mod}} T)}{\sqrt{2a} \cos(\omega_{\text{mod}} T) - 1}. \quad (3)$$

The spectrum of this field consists of discrete frequency sideband modes with separation ω_{mod} , and intensities that decrease following a geometric progression. For the particular case of the maximally-compressed solution of Eq. (3), the mode intensities are: $S_0 = P_0(2^{1/2}-1)^2$ for the pump, and $S_n = 2P_0(2^{1/2}-1)^{2|n|}$ (where $n = \pm 1, \pm 2, \pm 3, \dots$) for the sidebands. The pump and sideband intensities follow the relative progression $\{I_0, I_1, I_2, I_3, I_4, \dots\} = \{1, 2, 0.3431, 0.0589, 0.0101, \dots\}$. This geometric progression yields a characteristic triangular shape in the wings of the spectrum when plotted semi-logarithmically.

3. LINK TO SUPERCONTINUUM GENERATION EXPERIMENTS

We now present some experimental results: Fig. 1(a) shows spectral measurements at the output of 3.9 m of a highly nonlinear photonic crystal fiber with zero-dispersion wavelength at 780 nm for various peak powers using 1 ns pulses from a passively-modelocked microchip laser operating at 1064 nm. The experiment results in the top panel are compared with generalised nonlinear Schrödinger equation (GNLSE) simulations in the bottom panels. Full simulation details are to be found in Ref. [10] but we note that the major parameters were: $\beta_2 = -75 \text{ ps}^2 \text{ km}^{-1}$ and $\gamma = 60 \text{ W}^{-1} \text{ km}^{-1}$. The numerical techniques used are standard although we note that the nanosecond simulations did require extensive computational time at the highest peak powers. We stress that the simulations did model the full temporal envelope of these long pulses.

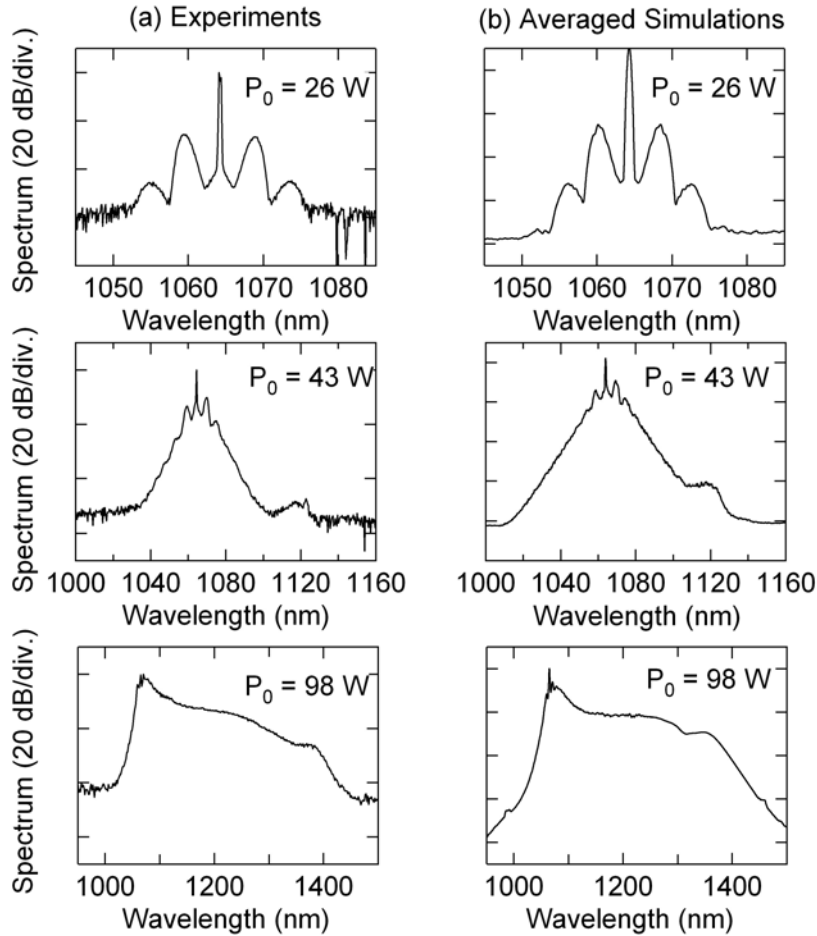


Fig. 1 Experimental results (left) and numerical simulation results (right) for 1 ns pulses at 1064 nm injected into highly nonlinear PCF at peak powers as shown. Note that the simulation results are averaged and convolved with a spectral resolution function matching the bandwidth of the spectrum analyzer used in the experiments (0.1 nm for 26 W results; 0.4 nm for 43 W results; 1.6 nm for 98 W results) [10].

We note immediately that the agreement between experiment and simulation is very good and illustrate the key steps of initial sideband development followed by the merging and formation of a continuous triangular pedestal about the pump. At the lowest power of 26 W, the spectrum consists of small number of distinct sidebands separated by the frequency of peak MI gain. As the power increases to 43 W, we enter an “extended MI” regime where we can still resolve sidebands close to the pump, but we also see the development of continuous low amplitude wings. These wings appear triangular when plotted with a semi-logarithmic y-axis and although this is a characteristic feature of this regime that we and many authors have noted in many years of experimental studies, this particular feature has thus far not been the subject of specific analysis or investigation. The spectral width in this regime approaches 60 nm at the -40 dB level, and we note the first sign of a very low amplitude Raman peak around 1120 nm. At higher power levels approaching 100 W (bottom), the characteristics of a “fully-developed” supercontinuum are observed [5]. In this case the spectrum extends significantly to longer wavelengths with features resembling soliton structures.

We focus now on the characteristics of the extended MI spectrum at 43 W peak power. In fact, although we have used GNLS simulations in Fig. 1(b), this power level actually describes a regime before the onset of higher-order effects become significant and thus is a parameter regime where we expect the AB theory (which is after all based on an NLSE system) to provide a good description. Moreover, we expect that the point of maximum spectral broadening within the framework of the AB evolution would correspond to the point where the temporal structure is maximally compressed. Or in other words, to the point where the spectrum would be modeled by the spectrum of the maximally-compressed AB pulse described above.

Indeed, we can confirm this using experimental spectral measurement by comparing the form of the measured spectrum with the geometric progression predicted for the maximally-compressed AB. Figure 2 compares numerical and analytic results with the experimental results of Fig. 1 for $P_0 = 43$ W. The numerical results show averaged multi-shot simulations using the full GNLSE with a 1 ns pulse input field (blue, short dashes) and using only the NLSE with a CW input field (red, long dashes). It is clear that both GNLSE and NLSE simulations produce similar results in agreement with experiment, with the GNLSE of course also predicting the onset of a small Raman peak on the long wavelength edge around 1120 nm; but this is largely insignificant in the context of the conclusions drawn here relating to AB dynamics. In fact these results also provide confirmation of the assumption that the spectrum at this point is explained by essentially NLSE dynamics.

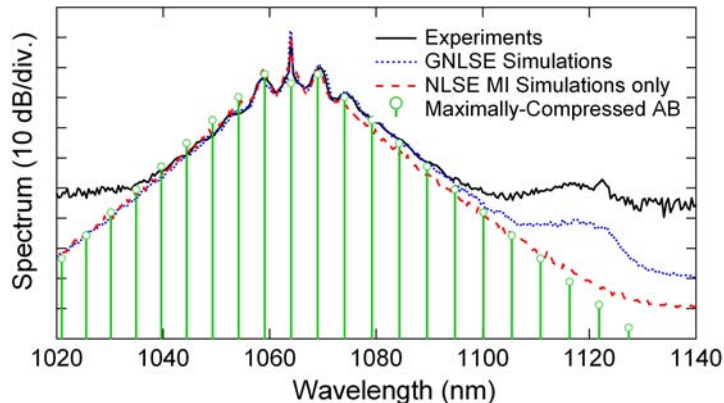


Fig. 2 Experiments (black line),simulations using the full GNLSE (blue dashed line), numerical simulations using the NLSE only (red dashed line), and the calculated spectrum of the maximally-compressed AB (green lines from zero) [10].

Perhaps the most important result here is the excellent agreement between the experimental decay of the spectral wings and the calculated amplitudes of the discrete frequency modes associated with the analytic form of the maximally-compressed AB. Because spontaneous MI is seeded by broadband noise, the spectral structure is of course not discrete, but rather consists of a continuous span of frequencies. Nonetheless, as with the time domain characteristics, we expect the spectral characteristics to contain a dominant component from the maximally-compressed AB solution calculated at peak MI gain. Thus, normalising to the $n = \pm 1$ sideband amplitudes of experiment, the decay of spectral intensity with frequency in experiment and simulations is reproduced very well by the analytic geometric progression of the maximally-compressed AB breather.

4. TURBULENCE DYNAMICS

These results suggest that the characteristics of emergent SC generation can be explained in terms of the development of high amplitude Akhmediev Breather sub-pulses. But of course this is not a complete explanation of how these sub-pulses subsequently separate from the extended MI spectrum and temporal pulse train and evolve towards higher-amplitude pulses that exhibit rogue wave statistics. In this context, however we note that any realistic optical fiber system would contain symmetry-breaking physical effects due to odd orders of chromatic dispersion and Raman scattering. In fact, both these effects are important in that they can induce collisions between the emergent breathers, but for illustrative purposes, we consider only the effect of third order dispersion in the results that follow. Recent work has also shown how the effect of third-order dispersion can lead to an additional form of convective instability [13].

The particular physical dynamics that we consider here involves the regime of soliton turbulence, where an initial phase of multiple soliton formation from a noisy background is followed by the emergence of a single large soliton that extracts energy from the background and acts as a statistical attractor. With this model, the initial phase of multiple soliton emergence is the AB regime considered in the previous section, and we now consider its longer time evolutionary limit. Understanding the intermediate phase of evolution is still an open problem.

We now consider the dynamics of soliton turbulence with an ideal cubic nonlinearity and only TOD perturbation and show that this leads to an appreciable growth of a single soliton. We consider different parameters here with input pulses duration of 10 ps (FWHM) and a propagation distance of 500 m. Periodic boundary conditions were imposed over a time window of 20 ps. Further details are given in [12]. Figure 3 shows the results obtained, plotting temporal intensity (top) and the corresponding spectrum (bottom) at selected distances of 20, 70, and 500 m. From the temporal trace it can be seen how a large-amplitude localized structure emerges from an ensemble of waves with significantly lower amplitude, and the emergence of this large-amplitude localized structure is correlated to the gradual broadening of the spectrum both on the long-wavelength and short-wavelength edges. With more detailed consideration of these results, we have found that the emerging large-amplitude pulse is well-fitted by a hyperbolic-secant profile and has soliton order near-unity, confirming the interpretation of a giant rogue soliton pulse emerging from and propagating amidst an otherwise low amplitude noise background.

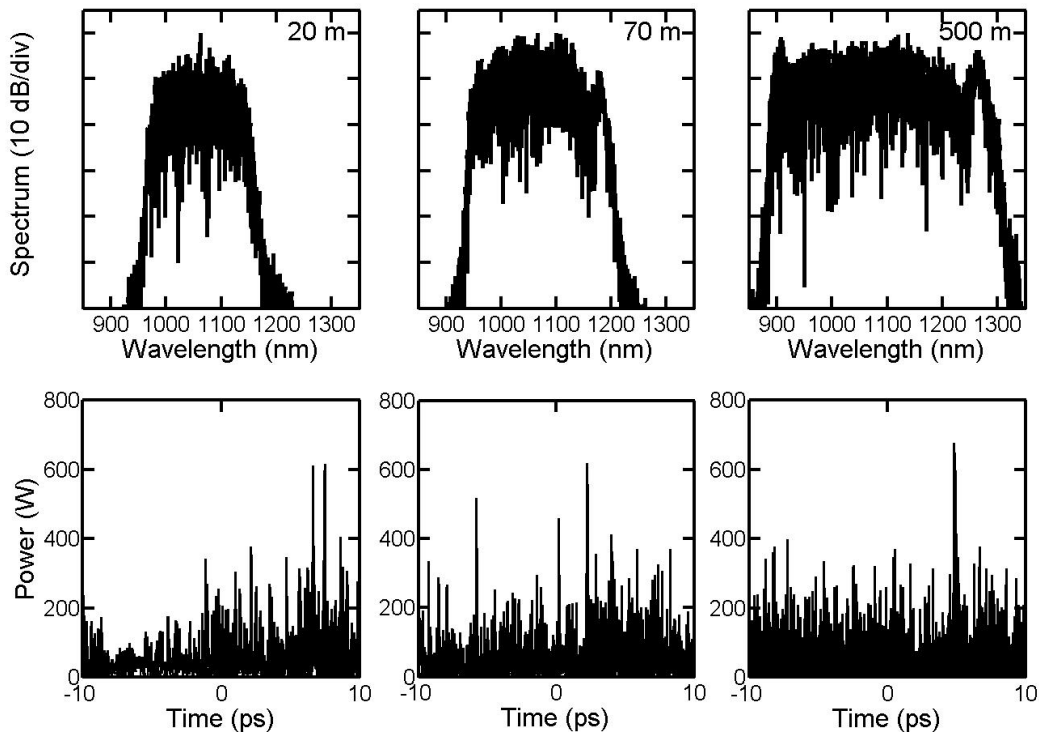


Fig. 3 Spectral (top) and temporal (bottom) profiles of evolving SC field at selected distances as shown in a long-distance limit with multiple collisions. Simulations use an NLSE with only TOD perturbation [12].

5. CONCLUSIONS

In conclusion, our numerical studies of spontaneous MI have shown that the well-known triangular form of the spontaneous MI spectrum when plotted semi-logarithmically can be explained naturally in terms of the analytic geometric progression describing the frequency dependence of AB modal amplitudes. In addition, other results have shown that SC generation described by an NLSE model perturbed only by TOD can lead to large amplitude localized optical rogue soliton and rogue wave structures. Generally speaking, any single perturbation that destroys the integrability of the NLSE is sufficient to observe “survival of the fittest” soliton amplification as a result of collisions. These results may have wide impact in improving understanding of the seeds of rogue wave formation in optics as well as hydrodynamics.

REFERENCES

1. D. R. Solli et al. "Optical rogue waves," *Nature* **450**, 1054-1057 (2007)
2. J. M. Dudley, G. Genty, B. J. Eggleton, "Harnessing and control of optical rogue waves in supercontinuum generation," *Opt. Express* **16**, 3644-3651 (2008)
3. M. Erkintalo, G. Genty, and J. M. Dudley, "Rogue wave like characteristics in femtosecond supercontinuum generation," *Opt. Lett.* **34**, 2468-2470 (2009)
4. G. P. Agrawal, *Nonlinear Fiber Optics*. 4th Edition. Academic Press, Boston (2007)
5. J. M. Dudley, G. Genty, and S. Coen, "Supercontinuum Generation in Photonic Crystal Fiber", *Rev. Mod. Phys.* **78**, 1135-1184 (2006)
6. N. Akhmediev, A. Ankiewicz, M. Taki, "Waves that appear from nowhere and disappear without a trace," *Phys. Lett. A* **373**, 675-678 (2009)
7. N. Akhmediev, J. M. Soto-Crespo, A. Ankiewicz, "Extreme waves that appear from nowhere: On the nature of rogue waves," *Phys. Lett. A* **373**, 2137-2145 (2009)
8. N. Akhmediev and V. I. Korneev, "Modulation instability and periodic solutions of the nonlinear Schrodinger equation," *Theor. Math. Phys.* **69**, 1089-1093 (1986)
9. J. M. Dudley, C. Finot, D. J. Richardson, G. Millot, "Self Similarity in Ultrafast Nonlinear Optics," *Nature Physics* **3** 597-603 (2007)
10. J. M. Dudley, G. Genty, F. Dias, B. Kibler, N. Akhmediev, "Modulation instability, Akhmediev Breathers and continuous wave supercontinuum generation," *Opt. Express* **17**, 21497-21508 (2009)
11. J. M. Dudley, G. Genty, F. Dias, B. Kibler, N. Akhmediev, Modulation Instability, Akhmediev Breathers and 'Rogue Waves' In *Nonlinear Fiber Optics SPIE Proceedings paper Vol. 7580*, Fiber Lasers VII, Technology, Systems and Applications (2010)
12. G. Genty, C. M. de Sterke, O. Bang, F. Dias, N. Akhmediev, J. M. Dudley "Collisions and turbulence in optical rogue wave formation," *Phys. Lett. A*, **374** 989-996 (2010)
13. M. Taki, A. Mussot, A. Kudlinski, E. Louvergneaux, M. Kolobov, M. Douay, "Third-order dispersion for generating optical rogue solitons," *Phys. Lett. A*, **374** 691-695 (2010)